WIRELESS COMMUNICATIONS AND MOBILE COMPUTING
Wirel. Commun. Mob. Comput. (2013)
Published online in Wiley Online Library (wileyonlinelibrary.com). DOI: 10.1002/wcm.2320

RESEARCH ARTICLE

Network properties of mobile tactical scenarios

Li Li[1], Phil Vigneron[1], Colin Brown[1], Thomas Kunz[2] and Weihua Zhuang[3]*

[1] Communications Research Centre Canada, Ottawa, Ontario, Canada
[2] Carleton University, Ottawa, Ontario, Canada
[3] University of Waterloo, Waterloo, Ontario, Canada

ABSTRACT

The mobile tactical network is a practical implementation of the mobile ad hoc network. Formed across tactical radios operating in the military very high frequency and low ultrahigh frequency bands, the mobile tactical network has distinctive characteristics when compared with generic mobile ad hoc networks, in particular with respect to its network topological behaviors and connectivity attributes. These characteristics must be understood and considered when selecting suitable network protocols. To this end, in this paper, a network science-based systematic modeling approach is applied to analyze typical deployment scenarios and identify fundamental tactical network properties. The novel framework employs realistic scenario models as well as radio physical layer performance parameters and channel models to effectively capture the dynamic network behavior that needs to be considered for protocol design. The results provide critical insights and guidance to the development of tactical network solutions. © Her Majesty the Queen in Right of Canada 2013

KEYWORDS
mobile tactical networks; mobility scenarios; network properties; network modeling

***Correspondence**
Weihua Zhuang, University of Waterloo, Waterloo, Ontario, Canada.
E-mail: wzhuang@uwaterloo.ca

1. INTRODUCTION

Tactical radios operating in the military very high frequency (VHF)/ultrahigh frequency (UHF) bands have been widely employed for real-time communications in challenging terrains, such as in rescue missions or on battle fields [1–3]. Leveraging multihop networking capabilities promised by mobile ad hoc networks (MANETs), a mobile tactical network [4–11] formed across tactical radios, may significantly improve communication coverage in the dynamic and dispersed mission-critical operational theater. The tactical network is also a typical deployment example of MANETs.

The tactical network is, however, very different from generic MANETs. For example, compared with generic WiFi radios used in MANETs, tactical radios in military VHF/UHF bands from 30 to 450 MHz often deliver a much lower link rate (e.g., from a few kilobits per second to a few hundred kilobits per second) and a much longer signal range (e.g., more than 10 km in complex terrains) [1–4]. This entails distinctive concerns when designing network protocols, as shown later in this work.

Networking schemes for tactical radios were studied as early as the 1980s [1–3]. These studies clearly identified that dynamic topology changes are detrimental to the performance robustness of networking protocols when operating on tactical radios. It is also noted that these early studies are very limited in applying network mobility scenarios, because of the lack of comprehensive mobility models at that time [12].

In the past two decades, solutions for MANETs that offer multihop capabilities have been intensely studied and also applied to tactical networks. However, most of the studies, even including those intended for tactical networks, assume high-bandwidth WiFi radios with a link rate of more than 1 Mbps, for example, 6–12 Mbps, and consequently a short range of only a few hundred meters in flat terrains [5–9,13,14]. The results are thus not very applicable to the tactical environment, where radios have different characteristics leading to different network topologies.

The effective design of network protocols requires understanding of both the network topological dynamics and the connectivity attributes exhibited in typical

deployment scenarios. Although comprehensive simulation platforms, models, and tools for mobile network scenario analysis have been developed [12,15–18], two critical aspects, which are often ignored, require much attention. First, physical radio link properties determine the topological and performance behavior of the network and thus cannot simply be assumed and abstracted out in the same way as was done in IP networks. For example, the topological dynamics and the data delivery performance of a network based on a disc model for radio signals [8,9] cannot resemble that of a real network whose link propagation never follows a simple on–off disc behavior [19]. It is thus essential to employ appropriate radio models so that a factual network topology can be obtained for protocol studies. Second, the deployment parameters applied in the network design and evaluation should be realistic. For instance, tactical networks rarely follow a random uniformly distributed mobility model, although such models, for example, the random waypoint model, are most popular in MANET studies. These studies then cannot validate the solution applicability in tactical scenarios [20].

To this end, in this paper, a novel approach that employs radio signal measurement data [21–23], practical deployment mobility models, and application parameters to study tactical network scenarios is taken. The focus is on the long-range, bandwidth-constrained tactical networks as they present an indispensable and yet most challenging case in tactical networking. In this paper, the term "tactical network" refers only to such long-range, bandwidth-constrained networks.

The contributions of this work are threefold:

(1) A novel systematic modeling approach is applied to analyze tactical network deployment scenarios using realistic radio and scenario parameters. This corrects the over-simplified assumptions that have been widely used in MANET scenario studies. The approach is also network protocol independent to discover inherent properties of the network without being limited by a pre-selected protocol scheme.
(2) Fundamental characteristics of the tactical network including its topological and connectivity attributes are identified.
(3) The obtained results point to important factors in protocol design for the tactical environment, elucidating critical issues and directions for potential solutions.

The rest of the paper is organized as follows. Section 2 describes the network parameters and the proposed network model. The network deployment scenario is presented and analyzed in Section 3. Section 4 illustrates the network properties obtained and explores them to evaluate some typical networking solution options. Section 5 briefly reviews the related work, and Section 6 finally concludes this research work.

2. MODELING MOBILE TACTICAL NETWORKS

The proposed network model integrates the conventional bottom and top layers of the network, namely, the physical radio layer and the user mobility and application parameters. These two layers, which are probably most distant from the networking layers in the middle, in fact drive the inherent topological and connectivity properties of the network. The observed fundamental network properties from the model are then, to some extent, independent of the network protocols, for example, medium access control (MAC) and routing. They intend to capture the best achievable statistical metrics as critical inputs to the selection and/or design of network protocols.

2.1. Network deployment requirements

Tactical networks have small to medium deployment sizes. Although a tactical network can scale up to 100 or 200 nodes in the future, it often consists of only 20–60 or even fewer nodes for operations on the run, much smaller than generic networks, for example, the fixed IP network. Instead of scalability, communication responsiveness, reliability, and robustness are primary concerns, quite different from the "best effort" service offered in most generic networks.

Despite very limited link capacity, the traffic of tactical communications is predominantly broadcast and multicast. Real-time voice has higher priority compared with other applications. Situational awareness information, for example, position data, generates typically small-sized data packets. The traffic profile has distinct patterns where commanders constantly communicate with their group(s). Network deployment scenarios often involve multiple groups of different roles, exhibiting a group-based mobility pattern.

2.2. Tactical radio links

The model starts from the radio links. Table I summarizes important variables and symbols used in this paper. A link between two radios is described by the probability of having the link given the signal propagation properties in the deployed terrain. A network of N nodes is thus modeled as an undirected time-variant geometric random graph $G_{P_1(t)}(N)$, where $P_1(t) = \left\{p_1^{(ij)}(t) | i, j = 1, 2, \ldots, N\right\}$ with $p_1^{(ij)}(t)$ being the link probability between nodes i and j (or j and i) at time t [24]. As the VHF and low-UHF links often show robust symmetric properties in both directions, the undirected graph assumption is reasonable, although the analysis can be extended straightforwardly to the directed case.

The link probability $p_1^{(ij)}(t)$ is determined by the radio signal propagation properties in the VHF/UHF tactical band [21–23]. The signal propagation loss is decomposed,

 DOI: 10.1002/wcm

Table I. Summary of variables and other symbols.

Symbols	Definition
N	Total number of nodes in the network
$p_{\mathrm{l}}^{(ij)}(t), p_{\mathrm{l}}^{(ij)}(k)$	Link probability between node i and j at time t, or at the kth sampling instant
$P_l(t), P_l(k)$	Network link probability matrix ($N \times N$) at time t, or at the kth sampling instant
$d_{ij}(t), d_{ij}(k)$	Distance between node i and j at time t, or at the kth sampling instant
TP_X	Transmission power
η	Path loss exponent
σ	Standard deviation of shadowing
$\alpha(d_0)$	Mean path loss at a reference distance d_0 in the far-field of the transmitter
S_p	Received power threshold for a required reception accuracy
p_{ls}	Frame transmission success probability across an existent link
R_{snr}	Received SNR
R_{X_NF}	Receiver noise floor
$\gamma_{\mathrm{v}}^{(ij)}(k)$	Voice path probability between node i and j at the kth sampling instant
$\Gamma_{\mathrm{v}}(k)$	Matrix of network voice path probability ($N \times N$) at the kth sampling instant
p_{dr}	Minimum voice packet end-to-end delivery ratio
ρ	Minimum path probability
$\gamma_{\mathrm{d}}^{(ij)}(k)$	Data path probability between node i and j at the kth sampling instant
$\Gamma_{\mathrm{d}}(k)$	Matrix of network data path probability ($N \times N$) at the kth sampling instant
$\gamma^{(ij)}(k)$	Highest possible path probability between node i and j at the kth sampling instant
$C_{\mathrm{N}}(k)$	Network connectivity level at the kth sampling instant
L_{m}	Path loss margin, $L_{\mathrm{m}} = TP_X - R_{X\_\mathrm{NF}} - R_{snr}$
av_nd	Label for "average node degree"
dh_	Label for "data path hop count"
dc_	Label for "data path spectral/send cost"
u	Network diameter
r	Lower bound on network node degree

on the basis of the signal measurement data obtained in the given band, into a path-loss component, a slow-varying local component of shadowing that has a log-normal distribution, and a fast-varying component with a Rician distribution. The Rician distribution is derived from VHF radio measurement data [23]. The VHF propagation often exhibits a dominant path between the transmitter and the receiver, such as a line-of-sight or a strong coherent component. Given the rather narrow channel bandwidth of tactical radios (e.g., 25 kHz), its envelope statistics are often well modeled by a Rician distribution, as shown in [23]. Even in urban environments, Rician fading is often observed, contrary to the conventional wisdom that urban areas exhibit primarily Rayleigh fading [23]. It is estimated that higher VHF and UHF band signals may exhibit a Rayleigh distribution more closely. However, the Rician model is reasonable considering that Rayleigh fading is a special case of Rician fading with the K-factor equal to zero.

A three-stage model is thus applied to describe the link: (1) the area mean depending on the path-loss characteristics in the range from the transmitter to the receiver; (2) shadowing within the receiving area with a log-normal distribution; and (3) instantaneous power superimposed with Rician fading.

The first component of the local area mean of received power at time t can be obtained as follows: $\xi(t) = TP_X - (\alpha(d_0) + 10\eta \log(d_{ij}(t)/d_0)), d_{ij}(t) > d_0$, where TP_X is the transmission power, $\alpha(d_0)$ is the mean path loss at a reference distance d_0 in the far-field of the transmitting antenna, $d_{ij}(t)$ is the distance between nodes i and j, and η is the path loss exponent.

The slow-varying shadowing component follows a log-normal distribution with a standard deviation. Then, the composite pdf for the instantaneous power of the desired signal Y at time t can be obtained as [24,25] follows:

$$f_Y(y,t) = \int_0^\infty \frac{(K+1)}{\sqrt{2\pi}\sigma x^2} \times \exp\left[-\frac{(K+1)\left(2y+s^2\right)}{2x} - \frac{(\ln x - \ln \xi(t))^2}{2\sigma^2}\right] \times I_0\left(\frac{\sqrt{2y}s(K+1)}{x}\right) \mathrm{d}x \quad (1)$$

where K is the Rician factor, $s = [2Kx/(K+1)]^{1/2}$, and I_0 is the modified Bessel function of the first kind. This leads to the following:

$$p_{\mathrm{l}}^{(ij)}(t) = \Pr\left(y(t) \geq S_p\right) = \int_{S_p}^\infty f_Y(y,t) = \mathrm{d}y \quad (2)$$

where S_p is the received power threshold for a required reception accuracy, given the background noise power.

 DOI: 10.1002/wcm

Although the MAC layer in a tactical network often employs a scheduling mechanism to handle hidden nodes and other interference issues, interference that cannot be controlled by the MAC (e.g., jammer attacks) will be present. Thus, interference is considered by an additional random noise added to the receiver noise floor, as shown in the computation of the model in Section 3.

In [21–23], signal measurements and empirical modeling are applied to characterize the propagation properties of VHF tactical channels. The aforementioned path characteristic parameters including α (d_0), η, and σ and Rician K factor are obtained for different types of terrain, which are employed in computing the model as to be shown in Section 3. Using tactical UHF channel measurement data, we can also directly apply the analysis to a UHF-based tactical network.

The link probability $p_1^{(ij)}(t)$ in (2) is a time-dependent variable, dependent on the distance metric $d_{ij}(t)$, which changes according to the network mobility model. To avoid over-simplified assumptions of node position distributions, realistic mobility scenario trace files are employed. The trace files can be gathered from operation exercises or produced by a mobility scenario generator, for example, the BonnMotion mobility generator [26]. The trace files contain the trajectory of each node by logging positions of the node through time. Then, given a set of time instants with sampling interval T, that is, $\{T, 2T, \ldots, WT\}$ where $W = \left\lfloor \frac{t_{max}}{T} \right\rfloor$, $0 < t \leq t_{\max}$, the position coordinates of all nodes in the network at each sampling instant kT, where $1 \leq k \leq W$, are collected in the position matrix $Q_{N\times 3}(k) = \{(q_{i1}(kT), q_{i2}(kT), q_{i3}(kT)) \,|i = 1, 2, \ldots, N, k = 1, 2, \ldots W\}$. A distance matrix is formed for all nodes at each sampling instant as $DS(k) = \{d_{ij}(k)|i, j = 1, 2, \ldots, N; k = 1, 2, \ldots, W\}$, where $d_{ij}(k) = \sqrt{\sum_{m=1}^{3} (q_{im}(kT) - q_{jm}(kT))^2}$.

Matrix $DS(k)$ is then applied to calculate the link probability at sampling instant kT. The network at time kT is thus captured by the $N \times N$ link probability matrix:

$$\mathrm{P_l}(k) = \left\{ p_1^{(ij)}(k) | i, j = 1, 2, \ldots, N, k = 1, 2, \ldots, W \right\}$$

With T sufficiently small, $\mathrm{P_l}(k)$ characterizes network links for the entire modeling duration.

The network receives frames instead of only a signal symbol or bit. The radio layer also has frame coding, protection, and recovery capabilities. Thus, in selecting the value for S_p in (2), the signal-to-noise ratio (SNR) determined by the required frame reception rate on each link is chosen, rather than the SNR for a simple bit error rate.

Denote the frame success probability across an existent link as p_{ls}. In analytical models, p_{ls} is often obtained by chaining the bit success rate on the basis of the packet/frame length [27]. A more realistic value for p_{ls} is however derived from the block/frame error rate measured on a typical tactical radio design. This is because the frame error/success rate is affected by various physical layer parameters, such as bandwidth, link transmission rate, error correlation, and coding rate, in addition to the packet/frame length. Figure 1 shows a sample of the frame error rate metric obtained by simulating typical tactical radio designs on the selected band, considering all key parameters such as modulation and coding [28]. Multiple design options of modulation and coding are evaluated to obtain realistic and yet not implementation-specific metric values. This approach gives a more accurate characterization of the radio physical layer for the network model, compared with other commonly used simplified frame/packet error rate calculations.

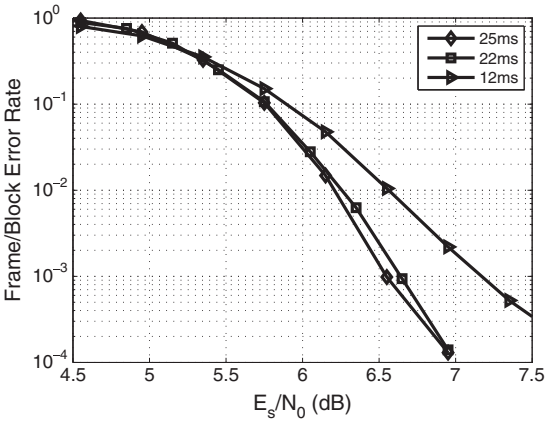

Figure 1. Radio performance data sample—continuous phase modulation, link rate 31.5 kbps, code rate 3/4, frequency 57.0 MHz, and bandwidth 25 kHz.

It is by selecting a required and yet achievable p_{ls} that the ratio of received energy per symbol to noise power spectral density (E_s/N_0) employed in the frame error measurement (Figure 1) can be mapped to the received SNR, denoted as R_{snr}, by using $R_{\mathrm{snr}} = \frac{E_s}{N_0} \times \frac{R_{\mathrm{b}}}{B} \times \frac{1}{CR}$, where R_{b}, B, and CR are transmission bit rate, bandwidth, and coding rate, respectively. Denoting the receiver noise floor as R_{X_NF}, we have $S_p = R_{\mathrm{snr}} \times R_{X\_\mathrm{NF}}$, where S_p is the signal threshold in (2). In this way, the S_p selected for calculating the link probability models the frame/packet delivery behavior.

2.3. The tactical network model

Given $p_1^{(ij)}(k)$, the average node degree can be obtained as

$$D_e(k) = 2 \sum_{i=1}^{N} \sum_{j=i+1}^{N} p_1^{(ij)}(k)/N \qquad (3)$$

For each given node i, its node degree is written as

$$D_e^{(i)}(k) = \sum_{j=1}^{N} p_1^{(ij)}(k) - 1 \qquad (4)$$

The probability that a link changes its state from sampling instant $(k-1)T$ to kT is calculated as

$$p_{\mathrm{lc}}^{(ij)}(k) = \left(1 - p_{\mathrm{l}}^{(ij)}(k-1)\right) p_{\mathrm{l}}^{(ij)}(k) + p_{\mathrm{l}}^{(ij)}(k-1)\left(1 - p_{\mathrm{l}}^{(ij)}(k)\right) \tag{5}$$

Now, for any node i, the expected number of its links that change states at time $t = kT$ is given by

$$E\left[LC_i(k)\right] = \sum_{j=1}^{N} p_{lc}^{(ij)}(k) \tag{6}$$

The path probability matrix of the network is computed to examine the network connectivity. The tactical network supports both voice and data, with real-time voice as the primary service. Real-time voice traffic requires paths of high availability and low latency. Retransmissions may not be performed at intermediate nodes even if errors occur in the reception. The path probability matrix for voice $\Gamma_{\mathrm{v}}(k)$, with the (i, j)th element $\gamma_{\mathrm{v}}^{(ij)}(k)$ defined as the voice path probability between node i and j at time $t = kT$, is computed assuming that the transmission from source to destination prefers all the intermediate hops to be available simultaneously and that the link and frame reception probabilities are independent on each transmission. A modified Floyd shortest path algorithm can be used to select the maximum path probability, as shown in Figure 2, at each sampling instant $t = kT, k = 0, 1, 2, \ldots, W$. It generates the voice path matrix $\Gamma_{\mathrm{v}}(k)$, covering all the nodes in the network through the entire network modeling duration. Other auxiliary data structures are used in the path computation algorithm to capture the list of hops contained along each path, which are not shown here to keep the descriptions succinct.

Voice can tolerate a small number of delivery errors. Denoting the minimum required delivery ratio of voice packets as p_{dr} and under the assumption of i.i.d. links, the path probability $\gamma_{\mathrm{v}}^{(ij)}(k)$ of the voice path between any two nodes i and j must satisfy $\gamma_{\mathrm{v}}^{(ij)}(k) \geq p_{\mathrm{dr}}/p_{\mathrm{ls}}^{h} = \rho$, where h is the number of hops the path traverses. With small p_{ls}, high p_{dr}, and/or large h, it may not be possible to achieve $\gamma_{\mathrm{v}}^{(ij)}(k) \geq \rho$, indicating that a path with the required delivery ratio p_{dr} does not exist in the network at the instant. Under this circumstance, Algorithm 1 as shown in Figure 2 returns the best possible path obtained, that is, the highest $\gamma_{\mathrm{v}}^{(ij)}(k)$. Different applications may require different p_{dr} values. In general, p_{ls} needs to attain a relatively high value in the multihop networking environment to achieve a high p_{dr}.

The path for data can differ from that for voice. Data communications tolerate end-to-end latency but not errors. Retransmission is used, for example, using a per-hop automatic repeat request scheme, to ensure reliable delivery. In this case, the "hop count" is formulated as the expected number of transmissions for the packet to traverse a hop. This hop count can be viewed as the path cost representing the spectral cost in terms of "number of sends," approximating the occupancy of spectrum. The probability that a packet is successfully received over a link between nodes i and j is $pp^{(ij)}(k) = p_{\mathrm{l}}^{(ij)}(k) \times p_{\mathrm{ls}}$. The expected total number of packet transmission attempts and ACKs over the link [27], which is the spectral cost of the hop, is

$$w_{\mathrm{s}}^{(ij)}(k) = \frac{1}{pp^{(ij)}(k)} + \frac{1}{\left(pp^{(ij)}(k)\right)^2} = \frac{1 + pp^{(ij)}(k)}{\left(pp^{(ij)}(k)\right)^2}.$$

The path matrix for data, $\Gamma_{\mathrm{d}}(k)$, with its (i, j)th element $\gamma_{\mathrm{d}}^{(ij)}(k)$, can thus be computed by using the algorithm in Figure 3.

Taking $\{k = 1, 2, \ldots, W\}$, Algorithms 1 and 2 generate the path matrices for voice and data at each sampling instant during the modeling time of the network. Given different path selection criteria, different path matrices can be computed by applying an appropriate optimization algorithm in a similar way. These path matrices generated are statistically the best possible paths that exist in the network, based on the selected path criteria, varying over time during the network operation. They represent topological attributes of the network based on the given radio and application parameters, independent of the routing protocols. A given protocol may or may not obtain the same paths depending on its path selection mechanism.

Input: $\mathrm{P}_l(k) = \left[p_l^{(ij)}(k)\right]$;
Output: $\Gamma_v(k) = [\gamma_v^{(ij)}(k)]$;

$\Gamma_v(k) = \mathrm{P}_l(k)$;
for m = 1 to N do
{
  for all i, j, do
    {
    If $(\gamma_v^{(ij)}(k) < \rho)$ $\gamma_v^{(ij)}(k) = \max\left(\gamma_v^{(ij)}(k), \gamma_v^{(im)}(k) \times \gamma_v^{(mj)}(k)\right)$;
    }
}
where ρ is the minimum path probability required to support the packet delivery ratio

Figure 2. Algorithm 1—voice path algorithm.

 DOI: 10.1002/wcm

Input: $W(k) = \left[w^{(ij)}(k)\right]$;

Output: $\Gamma_d(k) = \left[\gamma_d^{(ij)}(k)\right]$;

$\Gamma_d(k) = W(k)$;
for m= 1 to N do
{
for all i, j, do
{
$\gamma_d^{(ij)}(k) = \min\left(\gamma_d^{(ij)}(k),\ \gamma_d^{(im)}(k) + \gamma_d^{(mj)}(k)\right)$;
}
}

Figure 3. Algorithm 2—data path algorithm.

The majority of traffic in the tactical network consists of broadcast and multicast packets. To identify the path coverage conditions of the network under dynamic topology changes, the network connectivity level is evaluated in the model. The average network connectivity level $C_N(k)$ is defined as the ratio of the expected number of paths over the possible total number of paths (node pairs) in the network, given by

$$C_N(k) = \frac{2\sum_{i=1}^{N}\sum_{j=i+1}^{N}\gamma^{(ij)}(k)}{N \times (N-1)} \tag{7}$$

where $\gamma^{(ij)}(k)$ is the highest possible path probability between nodes i and j computed over all possible routes at the kth sampling instant. To obtain $\gamma^{(ij)}(k)$, the voice path computing algorithm (Algorithm 1) is applied with $\rho = 1$ to find the best path probability and thus statistically the highest connectivity level in the network at each sampling instant.

3. SCENARIO STUDIES

3.1. Radio and channel parameters

The models established in Section 2 are employed to analyze sample networks, given radio parameters as listed in Table II. The link transmission rates often vary in the field. The rate is lowered when a long-range signal is needed to reach a remote node. The transmission power is based on a vehicle-mounted unit. The receiver noise floor in the field is higher than the conventional value (e.g., −130 dBm) to incorporate the effect of interference.

Table II. Default radio parameters.

Description	Value (range)
Center frequency	57.0 MHz
Link rate	20–64 kbps
Noise floor	−126 to −95 dBm
Bandwidth	25 kHz
Transmit power	46 dBm
Frame length	12–25 ms

Table III. Path loss parameters (57.0 MHz, d_0 = 100 m).

Terrain	Semi-rural	Urban
Exponent η	3.18	4.31
Intercept α(100) (dB)	68.8	77.5
Std. dev. σ (dB)	4.11	6.41
Rician K factor	4.7	2.8

Considering some typical tactical voice codec, for example, NATO standard mixed-excitation linear prediction (MELPe) voice format, a sample voice packet is about 50 bytes long, including headers in a compressed format. This maps to a small frame duration of approximately 12 ms. Data traffic often consists of situational awareness information such as location data and short file/message exchange. The frame size for data varies from 12 to 25 ms [28]. Given the voice and data frame sizes, an achievable frame error rate for p_{ls} is 10^{-3}, as seen in Figure 1. Selecting $p_{ls} = 0.996$ in computing paths, the required SNR ranges from 4.25 to 23 dB, calculated using the frame error metric (e.g., Figure 1) and the method described in Section 2.2. A lower SNR usually is needed for a lower link rate and/or a higher SNR for higher link rate. On the basis of the voice application requirements, $p_{dr} \geq 96\%$ is chosen. The path loss margin (in dB) $L_m = TP_X - R_{X\_NF} - R_{snr} = TP_X - S_p$, is between 118 and 168 dB.

Two example scenarios are selected: a semi-rural and an urban terrain type. The path loss parameters obtained from the radio measurement data [21–23] are listed in Table III. The link probabilities in the two terrains are calculated and plotted in Figure 4, where the path loss margin is 140 dB for the semi-rural case and 144 dB for the urban case.

3.2. Scenario 1—semi-rural network deployment

The semi-rural environment where the signal propagation measurement data were taken has a significant amount of rural and forested areas, some overgrown farm fields and

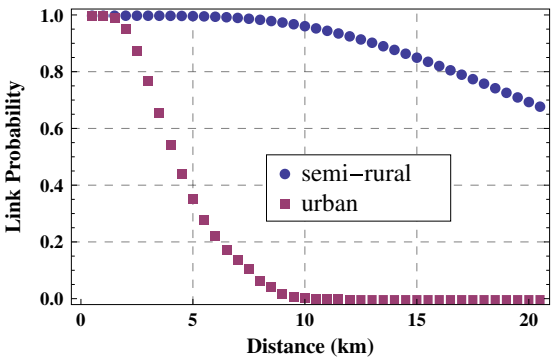

Figure 4. Link probabilities in the two deployment terrains.

a few two-story or three-story brick buildings [21–23]. The network has 38 deployed radio nodes in a 16 km by 16 km field, which is divided into four 8 km by 8 km non-overlapping quarters. Among all the nodes, three of them form a commander group positioned in a 4 km by 4 km area at the center of the field. A group of eight nodes is deployed in each of the four quarters. The mobility of commanders and the four groups follows the reference point group mobility model [17]. The remaining three nodes are individual nodes with assigned tasks such as reconnaissance or special operations. These three nodes move in the entire 16 km by 16 km field according to a random waypoint model. Except for the commander group, all the nodes travel at speeds in the range of 30–80 km/h, with an average pause time of 0–10 min. The commander group has an average pause time of 30 min and moves between speeds of 0 and 30 km/h. Within each group, the maximum distance from any node to the group center varies between 2 and 4 km. A total of 10 networks are generated to average the computation results. The modeling time for each network is 9000 s, and the sampling interval is chosen as $T = 3$ s, which is sufficient to capture the updates caused by the defined mobility in the given terrain.

From Figure 4, in this scenario, nodes less than 7 km apart can hear each other with a probability very close to 1. When nodes are farther apart, the link quality declines. Nodes within a group can mostly reach each other in one hop. Relays are needed to communicate across groups. The behavior is however far from a simple on–off disc model with a fixed radius.

The link probability matrix $P_{\mathrm{l}}(k) = \left[p_{\mathrm{l}}^{(ij)}(k)\right]$ at each sampling instant is obtained to compute various properties of the network. Figure 5 shows the distribution of node degree in the network for the SNR at the receiver varying from 12 to 23 dB, given $TP_X = 46$ dBm and average $R_{X\_\mathrm{NF}} = -107$ dBm. A higher SNR supports a higher link transmission rate. When the required SNR cannot be met at the receiver because of increased path loss and/or floor noise/interference, the link quality (probability) decreases.

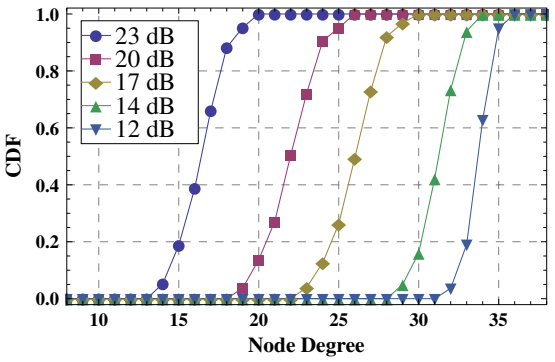

Figure 5. Distributions of node degree in the semi-rural scenario given required reception signal-to-noise ratio. CDF, cumulative distribution function.

Reducing the link transmission rate may then improve the link quality by lowering the SNR required for reception. The selected SNR values mostly correspond to link rates between 32 and 64 kbps, considering both voice and data frame sizes and parameters used in typical tactical radios.

In Figure 5, a higher SNR required at the receiver results in shorter signal range and smaller average network node degree, whereas a lower SNR needed for reception results in a longer signal range and higher average node degree. The average node degree varies from about 16.5–34 when the required SNR at the receiver changes 11 dB, or equivalently, when the path loss margin L_{m} changes 11 dB. These levels of node degree in the network are fairly high, indicating congested radio neighborhoods. Without losing connections in the network, one approach is to maintain a small node degree and relieve the neighborhood congestion by adjusting the link transmission rate (e.g., increasing the rate and thus reducing the signal range).

Network node degree is also closely related to the number of hops paths must traverse in the network. That is, it is related to the cost of network paths. Figure 6 shows the distribution of the network path cost, for both voice and data traffic, in relation to the average node degree in the network. In Figure 6, "av_nd" stands for "average node degree," "dh" is for data path hop count, and "dc" is for data path spectral/send cost. For node degrees ranging from 16.34 to 31.17, the network diameter varies from 9 to 3 for voice (Figure 6(a)). The network diameter for data varies from 5 to 2 in number of hops (solid lines in Figure 6(b)), which is smaller than that of voice, because data paths may employ retransmission for reliable delivery rather than using a path with more hops. The spectral cost of retransmission is, however, rather high (dashed line in Figure 6(b)), with a maximum value of more than 10 when the node degree is about 25.

Relay across multiple hops impedes performance by further reducing throughput on the low-rate links and increasing the end-to-end delay. More hops along a path also give rise to increased packet loss when any of the intermediate nodes moves and interrupts the path. The packet delivery performance often deteriorates with each added hop. Even with high quality links that have a link probability $p_{\mathrm{l}}^{(ij)} = 0.99$ and frame reception probability $p_{\mathrm{ls}} = 0.996$, a three-hop voice path will have a packet delivery ratio $p_{\mathrm{dr}} = \left(p_{\mathrm{l}}^{(ij)} \times p_{\mathrm{ls}}\right)^3 < 96\%$, failing to meet the application requirement. Thus, the network needs to have a small diameter. Maintaining such a closely connected network with a diameter of 3–4, the average node degree tends to be fairly high, at more than 25.

With lower node degree and increased number of path hops, the network connectivity level $C_{\mathrm{N}}(k)$, defined in (7), is reduced. The network connectivity level for the entire network modeling duration is plotted in Figure 7. When the node degree decreases to about 16, the network connectivity level can drop to lower than 80%. This takes place when the received SNR decreases about 10 dB, which can often happen in the field. The sharp decline happens

 DOI: 10.1002/wcm

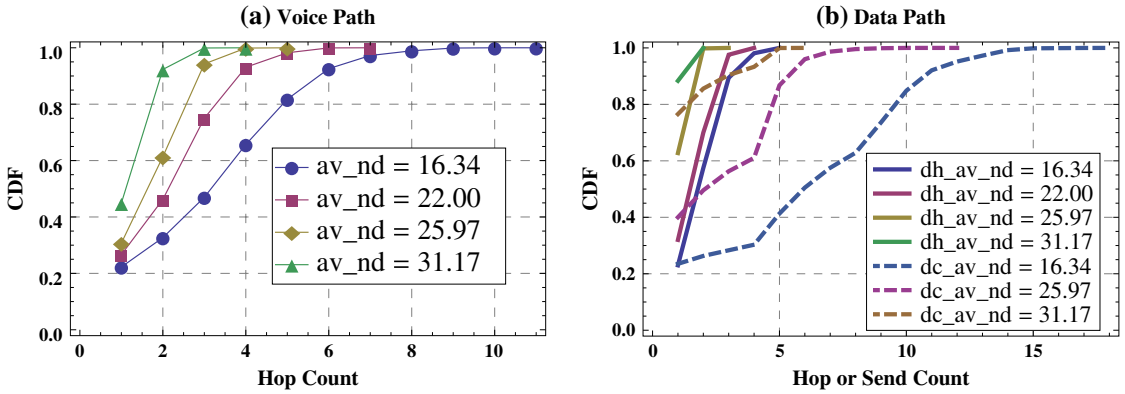

Figure 6. Path cost distributions in the semi-rural scenario. CDF, cumulative distribution function.

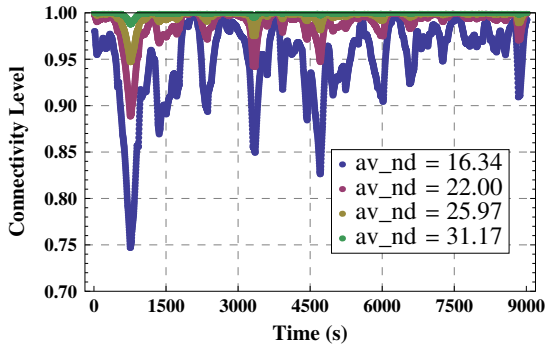

Figure 7. Network connectivity level in the semi-rural scenario.

Table IV. Path durations in scenario 1.

Stats	Group node	Commander node	Individual node
av_nd = 16.34			
Mean (s)	27.18	33.89	30.87
std. deviation	68.22	66.47	56.15
av_nd = 31.17			
Mean (s)	67.20	93.91	90.21
std. deviation	130.04	188.73	159.47

when an entire group is partitioned from the rest of the network, because of the group-based mobility model. The high SNRs selected, that is, from 12 to 23 dB to support a relatively high data rate from 32 to 64 kbps in the 25-kHz channel, also increase the sensitivity of the connectivity level. The network may either reduce link transmission rates to maintain a small network diameter and consequently high node degree or employ a multipath strategy to sustain the performance.

From the network path matrix, the path durations can be obtained. Table IV lists average durations and standard deviations for paths from different nodes to all other nodes in the network. Recall that the three commander nodes are in the middle of the network and the three individual nodes travel randomly in the entire network. An increased node degree stabilizes the paths and extends their duration. The deviations of the path durations are fairly large. Some of the paths, for example, the paths between nodes in the same group, stay unchanged for the entire network modeling duration of 9000 s. On the other hand, other paths may change frequently during a certain period. That is, a path may be stable for a while. Then, it starts to change, selecting a new hop in every sampling interval for a period, until it restabilizes. During the period of path churns, the path often lasts for less than 3 s. Significant packet delivery loss may be incurred if the routing protocol cannot keep up during the path churns. Again, increased node degree may improve the path duration at the expense of reduced link rate and aggravated radio neighborhood congestion. These issues and their implications on the network protocol design are further elaborated in the next section.

3.3. Scenario 2—urban network deployment

Urban canyons present the most challenging terrain for tactical networks. In this scenario, 38 nodes are deployed in a downtown area of 4 km by 4 km. All nodes follow the Manhattan grid mobility model [26], confined to streets separated by blocks of about 100 m in size. The measurement data taken from an urban environment are used in the models. The downtown area measured is heavily built containing 20-story glass and concrete buildings [23]. In addition, store fronts along some commercial streets have older brick construction of two stories. There were many vehicles in motion around the area where the measurement was taken. As shown in Figure 4, in a typical case with a path loss margin of 144 dB, the signal range extends to 1.2 km with a link probability very close to 1. At 3 km, the link probability declines to about 0.7.

Similarly to the previous scenario, three commander nodes are in the 1.2 km by 1.2 km central area of the field. Four groups are dispatched to the four non-overlap quarters of 2 km by 2 km in the 4 km by 4 km deployment field. In each group, two nodes are moving in the central 1 km by 1 km area of its quarter, whereas six others cover the entire assigned quarter. Three special operation nodes traverse within the entire deployment area along the streets. Although varying from time to time, an average traveling speed of 18 km/h is used for the commander nodes and 30 km/h for other nodes. The commander nodes may pause for 20 min while all other nodes may pause for 5–10 min in their movements.

The node degree distribution is presented in Figure 8. The cost distributions of voice and data paths are illustrated in Figure 9(a) and (b), respectively.

Compared with the semi-rural scenario, to maintain a similarly small network diameter of 3–4, the average node degree is found to be higher in the urban scenario, at around 29. In the urban environment, nodes experience severe path loss, leading to more hops/sends required for reachability. Again, the plots illustrate considerably higher spectral costs (dashed lines in Figure 9(b)) than the hop counts (solid lines in Figure 9(b)) in multihop data transmissions.

Although experiencing more path loss than the semi-rural scenario, the urban scenario shows less connectivity level degradation when the node degree decreases and the network diameter grows. With a 13-dB drop in the received SNR, for example, the lowest connectivity level holds at 84%. The reason is that the Manhattan grid model does not pull nodes into a close group, as was the case in the group reference model. Thus, compared with those in the previous scenario, the nodes here are more uniformly distributed, even though they are separated into groups in different quarters. A uniform node distribution sustains connectivity better under channel variations. The slower node traveling speed in the urban area also assists the connectivity. The path durations are longer than those in Scenario 1, except for the individual nodes, as shown in Table V. Again, although the average path durations are not very short, the path churns usually span several sampling time intervals. The individual nodes in this scenario have shorter path durations because of long and confined trajectories along the streets.

The node placement is critical in evaluating protocol performance. A protocol that performs well in more uniformly distributed deployments may not do as well in a group-based deployment. On the other hand, if it is possible to arrange node placements, a more uniform distribution should be attempted to enhance network endurance to channel variations.

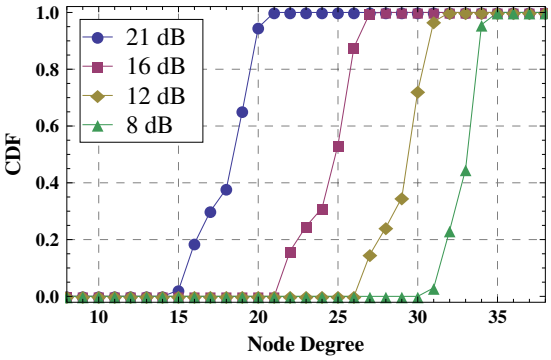

Figure 8. Distributions of node degree in the urban scenario given required reception signal-to-noise ratio. CDF, cumulative distribution function.

Table V. Path durations in scenario 2.

Stats	Group node	Commander node	Individual node
av_nd = 18.02			
Mean (s)	36.90	57.86	26.07
std. deviation	73.64	88.51	52.63
av_nd = 32.78			
Mean (s)	82.42	125.90	61.93
std. deviation	157.30	219.17	127.24

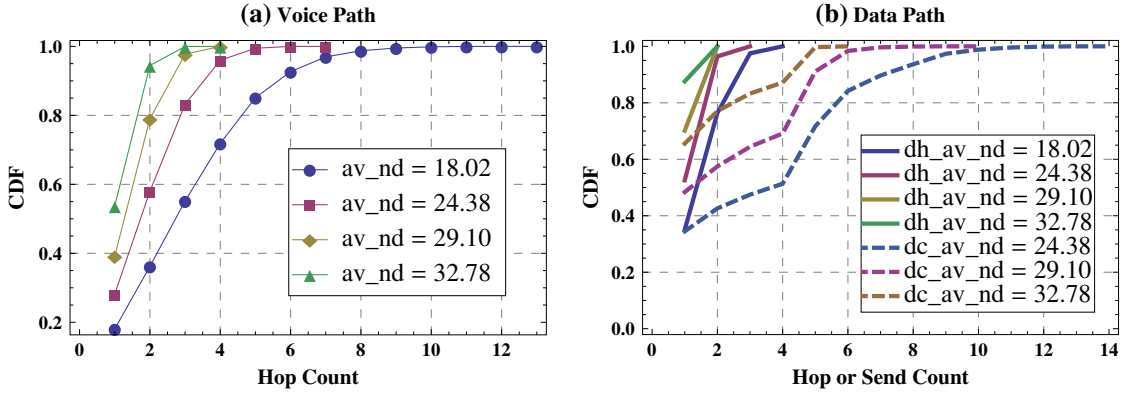

Figure 9. Path cost distributions in the urban scenario. CDF, cumulative distribution function.

 DOI: 10.1002/wcm

4. NETWORK PROPERTIES

4.1. The dense neighborhood

It has been observed from both scenarios that a fairly high average node degree is required in order to maintain a relatively small network diameter. In fact, from graph theory, to guarantee the network diameter at a given small value of u, the node degree must be fairly high. It is shown in [29] that for a given connected graph of N nodes and an integer u satisfying $N-1 > u > 2$, the node degree is bounded by r, such that if every node has its node degree $\geq r$, the diameter of the graph is at most u. The value of r is given by

$$r = \begin{cases} \left[\frac{N}{m}\right] & \text{if } u = 3m-4 \\ \left[\frac{N-1}{m}\right] & \text{if } u = 3m-3 \\ \left[\frac{N-2}{m}\right] & \text{if } u = 3m-2 \end{cases} \quad (8)$$

with $[x]$ denoting the largest integer not exceeding x and m an integer greater than 1.

The tactical network model assumes a geometric random graph rather than a general graph. In this case, with a network diameter upper bounded by u, the lower bound of the node degree tends to be higher. This can be seen as follows. It is shown in [29] that a graph can be formed as

$$\langle 1\rangle - \langle a_1\rangle - \langle a_2\rangle - \cdots - \langle a_{3_m-3}\rangle - \langle 1\rangle \quad (9)$$

where $\langle j\rangle$ denotes a nonempty complete subgraph with j nodes and $\binom{j}{2}$ edges. Two nodes in the different subgraphs in (9) have a direct link between them if and only if the two subgraphs are adjacent in the chain presentation. In the chain of (9), if the degree of each node is at least r, the diameter of the graph, which is the number of hops between the first and the last subgraph of the chain, is proven to be at most u. In the tactical network model, all links have a probability between "1" and "0" rather than being "1" or "0". For every two nodes i and j s.t. $i \in \langle a_1\rangle$ and $j \in \langle a_1\rangle$, the link between them must have a link probability $p_1^{(ij)}$ very close to 1 to ensure a diameter of u. Denote $p_1^{(ij)} \approx 1$, with $1 - p_1^{(ij)} = \delta$, where δ has to be very small, for example, $\delta < 0.01$ to ensure that the two end nodes are connected. Recall that link probability has to be higher than 0.99 for a three-hop path to have a packet reception ratio useful for voice applications, that is, to have two nodes "connected" in three hops, as discussed in the previous section. For the same reason, given any nodes $k \in \langle a_2\rangle$ and $q \in \langle a_3\rangle$, one has $1-p_1^{(ik)} = \delta$ and $1 - p_1^{(kq)} = \delta$, as the nodes are in neighboring subgraphs. It is by denoting the distance between any two nodes i and j as d_{ij} that $d_{iq} \leq d_{ik} + d_{kq}$ holds. From Figure 4, in the semi-rural terrain, to maintain $p_1^{(ik)} \approx 1$ and $p_1^{(kq)} \approx 1$, one has $d_{ik} \leq 7$ km and $d_{kq} \leq 7$ km. This leads to $d_{iq} \leq 14$ km. At 14 km, the link between node i and q has $p_1^{(iq)} > 0.8$, as seen from Figure 4. This shows that whereas in a general graph, the node degree of any node $i \in \langle a_1\rangle$ is $A_1 = 1 + (a_1 - 1) + a_2$ [29], in the geometric random graph here, the node degree of any node $i \in \langle a_1\rangle$ grows to be $A_1' > (1 + (a_1 - 1) + a_2)(1 - \delta) + 0.8a_3 = A_1(1-\delta)+0.8a_3$, considering nodes in $\langle a_1\rangle$ may even have weak links connecting nodes further than $\langle a_3\rangle$. Thus, for the networks considered here, $A_1' > A_1$ may easily hold. For example, even with a minimum $a_3 = 1$, $A_1' > A_1$ is true for $A_1 < 80$ and $\delta < 0.01$. Then, the following is true: In the tactical network model, for every subgraph in the chain of (9), any node in the subgraph will have a higher node degree when compared with the case of a general graph. It is also true for the case of urban terrain, where the link probability is close to "1" until nodes are 1.2 km apart and still maintains at about 0.87 when the distance expands to 2.4 km. Therefore, in the tactical network, to guarantee a network diameter u, the minimum node degree is generally higher than r given in (8). Thus, in theory, to guarantee a network diameter $u \leq 4$ in the network of 38 nodes, the minimum node degree must be 18.

This condition is sufficient but not necessary. It is possible to form a network with a diameter u where the minimum node degree in the network is smaller than r. In our experiments, the node degree observed however is rarely below r. Taking voice paths as an example, the conditions of node degree in relation to network diameter are shown in Table VI. To obtain the minimum and maximum node degrees, (4) is used to compute the node degree for each node at every sampling instant. Minimum node degrees much higher than r are often encountered.

The previous discussions demonstrate that in theory, the minimum node degree in the networks considered will be fairly high. High node degrees result in congested radio node neighborhoods. Networking protocols that apply two-hop neighborhood information collected via a periodic neighborhood discovery message such as HELLO [4–7,13,14,30] will incur increased overhead in such networks, because the message size and volume grow with the size of the neighborhood. As shown in [11], without counting any headers, HELLO message load reaches around 20 kbps in each node neighborhood in networks of scenario 1 that have a diameter of 3. Applying an efficient address compression on the HELLO message [31],

Table VI. Minimum node degree and network diameter.

Scenario	Diameter	Min. node degree	Max. node degree	r as given in (8)
1	3	25.2157	37.8958	18.5
	4	20.3962	37.6393	18
	5	14.1135	36.4172	12.67
2	4	23.072	37.5	18
	7	12.337	34.458	12

 DOI: 10.1002/wcm

the overhead on average still exceeds 6 kbps, excluding all headers. This occupies about 10% (higher in reality when counting headers needed for transmissions) of the 64-kbps bandwidth shared per neighborhood and thus may not be tolerable, considering that the link rate may need to decrease from time to time to maintain the network connectivity. Routing strategies for this type of tactical network thus may have to consider approaches based only on information of the one-hop neighborhood [10,11,32], unless the radio link rate can reach more than a few hundred kilobits per second.

Because of the high node degree, at least a few alternative relay nodes/paths exist between a source node and a destination node, with similar quality in terms of the end-to-end path probability. Note that voice paths may have difficulty to maintain the required packet reception ratio when multiple hops are involved. A multipath redundant delivery strategy may be applied to improve the delivery ratio and trade that off with increased spectral cost.

4.2. Path criticality and network hubs

When network node degree distributions are evaluated, the nodes in the center of the network are found to be network hubs, as they have a much higher node degree than other nodes. These nodes are also path critical nodes for the network, as many paths selected by common optimization algorithms, as shown in previous sections, traverse through them. This is much more pronounced in the semi-rural deployment scenario, where a group-based mobility model is applied. The three commander nodes have the highest node degree in the network and become path critical nodes. This illustrates a very congested radio neighborhood around the commander nodes. It also results in strong connectivity between the commander nodes and the rest of the network, with paths from the commander nodes to all other nodes in the network having mostly one hop, which may be desirable for supporting typical tactical traffic patterns.

The average voice path probability from any of the three commander nodes to all the other nodes in the network, referred to as the "commander's average path probability," is obtained from the voice path matrix computed at each sampling instant. It is found that the commander's average path probabilities are closely related to the average network connectivity level $C_N(k)$. In Figure 10, one commander's average path probability is plotted together with the network connectivity level $C_N(k)$ for scenario 1, to illustrate this observation. Similar observations hold for other commander nodes in scenario 1 although are much less pronounced in scenario 2. Such a match is not found for any other nodes in the network.

The phenomenon shows that a hub node has a global view of the network overall connectivity by simply observing its own connectivity conditions with the rest of the network. On one hand, the hub nodes are path critical nodes that assume relay duties for many paths, a situation

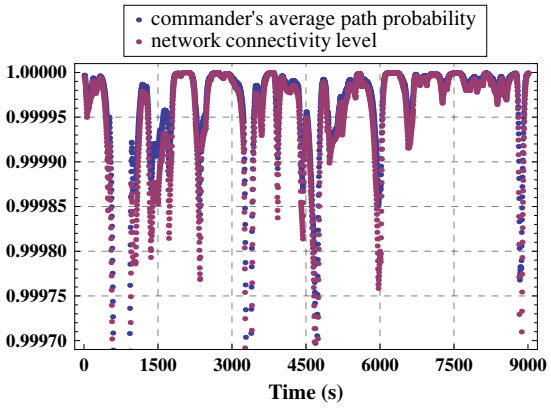

Figure 10. Network connectivity level versus commander's average path probability.

that creates critical paths, vulnerability, and bottlenecks in the network. Thus, a routing algorithm should carefully apply optimization criteria to avoid overloading the critical nodes. On the other hand, the hub nodes can be good candidates for network connectivity monitoring functions to evaluate the entire network reachability status.

4.3. Link dynamics

The dynamic link changes in the network can be captured using (5) and (6). Figure 11 illustrates the distribution of the percentage of links that change their states across each sampling interval. For example, with node degrees of 16 and 18 in the semi-rural and urban cases, respectively, on average, about 23% and 25% of the links in the network experience state changes in a 3-s sampling interval. This amounts to about 160 reports of 80 links changing their state at a given time in the network, and every node has at least one link change across each sampling interval. The urban scenario experiences higher link dynamics than

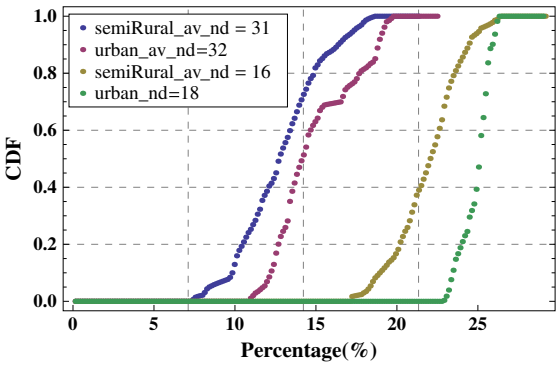

Figure 11. Percentage of link state changes per sampling interval.

 DOI: 10.1002/wcm

the semi-rural scenario. A higher node degree stabilizes the link status in both cases.

The frequent link state updates may engender extensive link status reports in many quality of service (QoS)-based routing schemes. Because of the high reliability required and the relatively high packet loss ratio on the radio links, QoS routing may be necessary. However, the link status update cost and the instability of the overall link status in the view of each node need to be considered. Additionally, path churns as identified in the previous section may force path selection to take place frequently (e.g., every 3 s) in a certain period. This demands highly up-to-date link status and more frequent update reports. Reporting link status updates in the network to achieve QoS routing can thus be very costly and not sustainable. These findings have led us to a different approach where only a few critical links need to report their status updates. The network hub nodes are leveraged to observe the link changes without invoking reports from many other nodes when links are symmetric. Simulation results from this new approach show improved path QoS with reduced and well-contained link update overhead [33].

5. RELATED WORK

Investigating network fundamental behaviors to assist network system design has drawn attentions lately [15,16,18]. Many of the studies have been focused on analysis of interactions between users and networks to improve the overall network behavior prediction and control [15,16]. A new system framework and extensive tools for adaptive protocol design and scenario analysis have been proposed [15,18]. However, few reports have analyzed mobile tactical networks with a focused consideration of physical layer effects to identify various critical factors that impact the overall network topology and performance. Even in tactical scenario studies [18], only short-range high-UHF and high-bandwidth radios, which are very different from the tactical radios operating on VHF and low-UHF bands, are considered.

Studies of basic characteristics of MANETs have been conducted in the past and have resulted in analytical models that capture the link probability, the stability distribution of links [34,35], and other network properties (e.g., connectivity) [36,37]. In [37], given the node's maximum transmission range, the number of nodes required to cover a certain area with a k-connected network was found. Results on node degree distribution and network max-flow capacity were also presented. However, these analytical models assume a random uniform distribution of nodes and a simple link model of disc signal coverage and suffer from border effects. Although providing good theoretical benchmarks, they do not consider specific tactical network scenarios, deployment conditions, or channel properties. Their applicability in providing guidance to tactical network protocol design may thus be quite limited.

Another large body of related work in the area of MANETs includes extensive protocol design and simulation effort [4–9,13,14] where network scenarios were established for mission-critical MANETs, which to some extent may be close to the tactical network discussed in this study. Besides using generic WiFi radio (e.g., IEEE 802.11) models in the studies, the simulations are mostly specific to a particular implementation of each of the different layers and do not easily generate detailed measurements of basic network properties. In this work, we have leveraged and applied the advances of simulations for MANET, especially in employing various mobility models that are very applicable to different segments in the tactical deployment to compose tactical mobility scenarios.

In tactical networks, node mobility is often not random, nor are the nodes uniformly distributed; a simple link model is also inadequate as link properties in the mobile radio networks have become much more critical, impacting overall network performance. In [10,38], a preliminary version of the network model of this work was presented and applied in selecting network protocol design options. In the previous work reported in [10,38], the channel model was incomplete without considering the fast-fading component, and only very limited scenario cases were explored. This work completes the network model and establishes the empirical results for the fundamental network properties of tactical networks to identify critical issues, challenges, and potential directions in the network solution design.

6. CONCLUSIONS

This paper presents a new network modeling approach to study the fundamental properties of tactical networks in typical deployment scenarios. The approach employs realistic physical and scenario layer parameters and geometric random graphic models to identify network behaviors. It is found that radio and scenario parameters significantly affect the network properties, for example, path hop count distributions, network diameters, network connectivity levels, and path duration distributions. Therefore, the simplified assumptions on radio signal range models and node mobility distributions that have been widely used in network protocol studies may easily fail to engender robust networking schemes for the tactical environment.

The results point to very high radio neighborhood density and congestion levels in the tactical network. They also illustrate very intensive link and path dynamics at times, such as path churns in a short period even though the path durations are, in general, much longer. This leads to possible excessive overhead cost for popular networking protocols when updating two-hop neighbor information and when updating link status for QoS improvements. Even so, the node degree may still not be high enough to maintain network connectivity and required packet delivery ratio along multihop paths when the received SNR fluctuates. These findings highlight the need to apply alternative options such as selected critical link update schemes

  DOI: 10.1002/wcm

and multipath redundancy delivery strategies for QoS routing, for example. The results also provide important guidance in selecting parameters for network operations, for instance, path loss margins and link transmission rates, to sustain robust performance. In our current work, tactical networking protocols are being devised on the basis of the understanding of the dynamic network behaviors gathered from this study to achieve enhanced network reliability and performance.

ACKNOWLEDGEMENT

This work is supported by the Defence Research and Development Canada.

REFERENCES

1. Lewis M, Garcia-Luna-Aceves J. Packet-switching applique for tactical VHF radios. *Proceedings of IEEE MILCOM, 1987* 1987; **2**: 0449–0455. DOI: 10.1109/MILCOM.1987.4795249.
2. Davies BH, Davies TR. The application of packet switching techniques to combat net radio. *Proceedings of the IEEE* 1987; **75**(1): 43–55. DOI: 10.1109/PROC.1987.13704.
3. Jubin J, Tornow JD. The DARPA packet radio network protocols. *Proceedings of the IEEE* 1987; **75**(1): 21–32. DOI: 10.1109/PROC.1987.13702.
4. Wang H, Crilly B, Zhao W, Autry C, Swank S. Implementing mobile ad hoc networking (MANET) over legacy tactical radio links, In *Proceedings of IEEE MILCOM 2007*, Orlando, Florida, 2007; 1–7, DOI: 10.1109/MILCOM.2007.4455103.
5. Blair A, Brown T, Chugg KM, Johnson M. Tactical mobile mesh network system design, In *Proceedings of IEEE MILCOM 2007*, Orlando, Florida, 2007; 1–7, DOI: 10.1109/MILCOM.2007.4454980.
6. Fossa CE, MacDonald TG. Internetworking tactical MANETs, In *Proceedings of IEEE MILCOM'10*, San Jose, California, 2010; 611–616, DOI: 10.1109/MILCOM.2010.5680456.
7. Demers S, Kant L. MANETs: performance analysis and management, In *Proceedings of IEEE MILCOM 2006*, Washington, DC, 2006; 1–7, DOI: 10.1109/MILCOM.2006.302055.
8. Gohari AA, Pakbaz R, Rodoplu V. RMR: reliability based multi-hop routing in wireless tactical networks, In *Proceedings of IEEE MILCOM'10*, San Jose, California, 2010; 995–1001, DOI: 10.1109/MILCOM.2010.5679570.
9. Sagduyu YE, Song L, Jason HL. On the overhead and throughput performance of scent-based MANET routing, In *Proceedings of IEEE MILCOM'10*, San Jose, California, 2010; 977–982, DOI: 10.1109/MILCOM.2010.5679577.
10. Li L, Kunz T. Efficient mobile networking for tactical radios, In *Proceedings of IEEE MILCOM'09*, Boston, MA, 2009; 1–7, DOI: 10.1109/MILCOM.2009.5380133.
11. Li L, Kunz T. Efficiency of multiparty networking protocols over mobile tactical radios on VHF bands, In *Proceedings of IEEE MILCOM'10*, San Jose, CA, 2010; 1110–1115, DOI: 10.1109/MILCOM.2010.5680089.
12. Camp T, Boleng J, Davies V. A survey of mobility models for ad hoc network research. *Wireless Communication and Mobile Computing (WCMC)* 2002; **2**(5): 483–502.
13. Pei G, Gerla M, Hong X. LANMAR: landmark routing for large scale wireless ad hoc networks with group mobility, In *Proceedings of IEEE/ACM MObiHoc*, Boston, MA, 2000; 11–18, DOI: 10.1109/MOBHOC.2000.869208.
14. Qayyum A, Viennot L, Laouiti A. Multipoint relaying: an efficient technique for flooding in mobile wireless networks. *INRIA Research Report RR-3898*, 2000.
15. Kant L, Yong K, Younis O, Shallcross D, Sinkar K, Mcauley A, Manousakis K, Chang K, Graff C. Network science based approaches to design and analyze MANETs for military applications. *IEEE Communications Magazine* 2008; **46**(11): 55–61. DOI: 10.1109/MCOM.2008.4689245.
16. Gharai L, Guan K, Ghanadan R. Military scenarios and solutions from a network science perspective, In *Proceedings of IEEE MILCOM'09*, Boston, MA, 2009; 1–6, DOI: 10.1109/MILCOM.2009.5379858.
17. Hong X, Gerla M, Pei G, Chiang CC. A group mobility model for ad hoc wireless networks, In *Proceedings of ACM MSWiM'99*, Seattle, WA, 1999; 53–60, DOI: 10.1145/313237.313248.
18. Kaplan MA, Chen T, Fecko MA, Gurung P, Hokelek I, Samtani S, Wong L, Patel M, Staikos A, Greear B. Realistic wireless emulation for performance evaluation of tactical MANET protocols, In *Proceedings of IEEE MILCOM'09*, Boston, MA, 2009; 1–7, DOI: 10.1109/MILCOM.2009.5379957.
19. Herms A, Lukas G, Ivanov S. Realism in design and evaluation of wireless routing protocols, In *Proceedings of Workshop on Mobile Services and Personalized Environments*, Aachen, Germany, 2006; 57–70.
20. Burbank JL, Chimento PF, Haberman BK, Kasch WT. Key challenges of military tactical networking and the elusive promise of MANET technology. *IEEE Communications Magazine* 2006; **44**(11): 39–45. DOI: 10.1109/COM-M.2006.248156.

  DOI: 10.1002/wcm

21. Pugh J, Bultitude R, Vigneron P. Path loss measurements with low antennas for segmented wideband communications at VHF, In *Proceedings of IEEE MILCOM'06*, Washington, DC, 2006; 1–5.
22. Pugh J, Bultitude R, Vigneron P. Propagation measurements and modelling for multiband communications on tactical VHF channels, In *Proceedings of IEEE MILCOM'07*, Orlando, FL, 2007; 1–5.
23. Vigneron P, Pugh J. Propagation models for mobile terrestrial VHF communications, In *Proceedings of IEEE MILCOM'08*, San Diego, CA, 2008; 1–7, DOI: 10.1109/MILCOM.2008.4753160.
24. Hekmat R. *Ad-hoc Networks: Fundamental Properties and Network Topologies*. Springer: The Netherlands, 2006. 25–35.
25. Prasad R, Kegel A. Effects of Rician faded and Log-Normal shadowed signals on spectrum efficiency in microcellular radio. *IEEE Transactions on Vehicular Technology* 1993; **42**(3): 274–281.
26. Aschenbruck N, Ernst R, Gerhards-Padilla E, Scheamborn M. BonnMotion—a mobility scenario generation and analysis tool, In *Proceedings SIMUTools'10*, Torremolinos, Spain, 2010; (51). DOI: 10.4108/ICST.SIMUTOOLS2010.8684.
27. Kuruvila J, Nayak A, Stojmenovic I. Hop count optimal position-based packet routing algorithms for ad hoc wireless networks with a realistic physical layer. *IEEE JSAC* 2005; **23**(6): 1267–1275.
28. Brown C, Pugh J, Vigneron P. Design considerations and performance of networks narrowband waveforms for tactical communications, In *Proceedings of NATO IST-092 Symposium on Military Communications and Networks*, Poland, 2010.
29. Moon JW. On the diameter of a graph. *Michigan Mathematical Journal* 1965; **12**(3): 349–351.
30. Clausen T, Jacquet P. Optimized link state routing protocol (OLSR). *IETF RFC 3626*, 2003.
31. Clausen T, Dearlove C, Dean J, Adjih C. Generalized mobile ad hoc network (MANET) packet/message format. *IETF RFC 5444*, 2009.
32. Kwon TJ, Gerla M, Verma VK, Barton M, Hsing TR. Efficient flooding with passive clustering—an overhead-free selective forwarding mechanism for ad hoc/sensor networks. *Proceedings of IEEE* 2003; **91**(9): 1210–1220.
33. Li L, Shi M, Kunz T. Robust networking for bandwidth constrained mobile tactical radios, In *Proceedings of IEEE VTC Spring*, Yokohama, Japan, 2012; 1–5, DOI: 10.1109/VETECS.2012.6240025.
34. Wu X, Sadjadpour HR, Garcia-Luna-Aceves JJ. Routing overhead as a function of node mobility: modeling framework and implications on proactive routing, In *Proceedings of IEEE MASS*, Pisa, Italy, 2007.
35. Han Y, La RJ, Zhang H. Path selection in mobile ad-hoc networks and distribution of path duration, In *Proceedings of IEEE Inforcom'06*, Barcelona, Spain, 2006; 1–12, DOI: 10.1109/INFOCOM.2006.11.
36. Bettstetter C. On the minimum node degree and connectivity of a wireless multihop network, In *Proceedings of ACM MobiHoc'02*, Lausanne, Switzerland, 2002; 80–91, DOI: 10.1145/513800.513811.
37. Fan P, Li G, Cai K, Letaief KB. On the geometrical characteristics of wireless ad-hoc networks and its application in network performance analysis. *IEEE Transactions On Wireless Communications* 2007; **6**(4): 1256–1265. DOI: 10.1109/TWC.2007.348322.
38. Li L, Vigneron P. Properties of mobile tactical radio networks on VHF bands, In *Proceedings of NATO IST-092 Symposium on Military Communications and Networks*, Poland, 2010.

AUTHORS' BIOGRAPHIES

Li Li (li.li@crc.gc.ca) received her PhD in Electrical Engineering from University of Ottawa, Canada, in 1993. She then worked with Nortel Networks as a system architect and a product manager. In 1999, she joined SS8 Networks as the chief product architect. Since 2003, she has been a research scientist in the Communications Research Centre (CRC) Canada. Her research interests include networking protocols and adaptive systems. Her current work focuses on tactical communications networks. She is an Associate Editor for IEEE Transactions on Vehicular Technology and for Springer's Journal on Peer-to-Peer Networking and Applications and is also involved in international conferences.

Phil Vigneron (phil.vigneron@crc.gc.ca) received his PhD in Electrical Engineering from Queen's University, Canada, in 1999. He is a research scientist in the Communications Research Centre, a federal government research lab in Canada. His area of interest is wireless communications, especially modulation, coding, radio propagation, and robust waveform design for military applications. His current work is on topics supporting the development of wireless network connectivity on the battlefield.

Colin Brown (colin.brown@crc.gc.ca) received his PhD in Electronics from the University of York, UK, in 2001. In 2001, he joined Nortel Networks in the advanced wireless group as a researcher. Since 2003, he has been with the Terrestrial Wireless Systems Group of the Communications Research Centre (CRC) Canada. His interests include signal processing and communication systems.

Thomas Kunz (tkunz@sce.carleton.ca) received the Dr. Ing. degree in Computer Science in 1994, from the Darmstadt University of Technology, Federal Republic of Germany. He is currently a professor in Systems and Computer Engineering at Carleton University. His research interests are in the area of wireless and mobile computing. He co-authored over 150 refereed papers, received a number of awards, and is involved in national and international conferences and workshops.

Weihua Zhuang (wzhuang@uwaterloo.ca) has been with the Department of Electrical and Computer Engineering, University of Waterloo, Canada, since 1993, where she is a professor and a Tier I Canada Research Chair in Wireless Communication Networks. Her current research focuses on resource allocation and QoS provisioning in wireless networks. She is a co-recipient of the Best Paper Awards from the IEEE Multimedia Communications Technical Committee in 2011, IEEE Vehicular Technology Conference (VTC) Fall 2010, IEEE Wireless Communications and Networking Conference (WCNC) 2007 and 2010, IEEE International Conference on Communications (ICC) 2007, and the International Conference on Heterogeneous Networking for Quality, Reliability, Security and Robustness (QShine) 2007 and 2008. She received the Outstanding Performance Award four times since 2005 from the University of Waterloo and the Premier's Research Excellence Award in 2001 from the Ontario Government. Zhuang is the Editor-in-Chief of IEEE Transactions on Vehicular Technology and the Technical Program Symposia Chair of the IEEE Globecom 2011. She is a Fellow of the IEEE, a Fellow of the Canadian Academy of Engineering (CAE), a Fellow of the Engineering Institute of Canada (EIC), and an elected BoG member of IEEE Vehicular Technology Society.

 DOI: 10.1002/wcm